nature geoscience

ARTICLES

https://doi.org/10.1038/s41561-020-0552-y

Multiple early-formed water reservoirs in the interior of Mars

Jessica J. Barnes[1,2]✉, Francis M. McCubbin[1], Alison R. Santos[3], James M. D. Day[4], Jeremy W. Boyce[1], Susanne P. Schwenzer[5], Ulrich Ott[6,7], Ian A. Franchi[5], Scott Messenger[1], Mahesh Anand[5,8] and Carl B. Agee[9]

The abundance and distribution of water within Mars through time plays a fundamental role in constraining its geological evolution and habitability. The isotopic composition of Martian hydrogen provides insights into the interplay between different water reservoirs on Mars. However, D/H (deuterium/hydrogen) ratios of Martian rocks and of the Martian atmosphere span a wide range of values. This has complicated identification of distinct water reservoirs in and on Mars within the confines of existing models that assume an isotopically homogenous mantle. Here we present D/H data collected by secondary ion mass spectrometry for two Martian meteorites. These data indicate that the Martian crust has been characterized by a constant D/H ratio over the last 3.9 billion years. The crust represents a reservoir with a D/H ratio that is intermediate between at least two isotopically distinct primordial water reservoirs within the Martian mantle, sampled by partial melts from geochemically depleted and enriched mantle sources. From mixing calculations, we find that a subset of depleted Martian basalts are consistent with isotopically light hydrogen (low D/H) in their mantle source, whereas enriched shergottites sampled a mantle source containing heavy hydrogen (high D/H). We propose that the Martian mantle is chemically heterogeneous with multiple water reservoirs, indicating poor mixing within the mantle after accretion, differentiation, and its subsequent thermochemical evolution.

Mars is composed of a core, mantle, crust and atmosphere, and this basic structure is the sum effect of its accretion, differentiation and subsequent thermochemical evolution. The initial abundance, distribution and isotopic composition of water within these structural components is poorly constrained, but important insights have been gained from analysis of Martian meteorites, telescopic observations and launched missions to Mars, including Mars-orbiting spacecraft, landers and rovers[1]. Data from all of these efforts indicate that there are at least two isotopically distinct water reservoirs on Mars. One reservoir, thought to reside in the atmosphere and within surficial polar ice deposits, is characterized by a D/H ratio that is elevated relative to Vienna Standard Mean Ocean Water (VSMOW, 1.56×10^{-4}) by a factor of 5 to 7 (refs. [2–4]), which is attributed to hydrogen loss over time from the upper atmosphere of Mars in the absence of a persistent and long-lived global magnetic field[5]. The second is thought to represent the primordial Martian mantle with a D/H ratio of $(1.99\pm0.02)\times10^{-4}$, which is enriched relative to VSMOW by a factor of 1.3 (ref. [6]). Analyses of hydrous phases in Martian meteorites and in situ analyses of materials on the Martian surface yield a wide range of D/H values that largely sit between these two endmembers[7,8], so many previous studies have implicated mixing of these reservoirs and/or terrestrial contamination to explain the observed variations in D/H ratios. However, Mars lacks unambiguous evidence of once having Earth-style plate tectonics, and in the absence of plate tectonics, the crust acts as a physicochemical barrier between the atmosphere and mantle; hence, it is a critical part of constraining any mixing model between the atmosphere and mantle reservoirs. Moreover, the H-isotopic composition of the Martian crust remains poorly characterized, despite its being a major water reservoir on Mars[9], which has impeded any systematic evaluation of proposed mixing models between the atmosphere and mantle. Here we have characterized the H-isotopic composition of the Martian crust over the time span of 3.9–1.5 billion years ago (Ga) using samples that are known to have interacted with Martian crustal fluids, including Allan Hills (ALH) 84001 and Northwest Africa (NWA) 7034.

Isotopic signature of water in the Martian crust

ALH84001 is an orthopyroxenite that crystallized in the crust ~4.1 Ga (refs. [10,11]) and experienced hydrothermal alteration with crustal fluids at about 3.9 Ga (ref. [12]). NWA7034 and its pairings represent a regolith breccia of basaltic bulk composition[13] that was lithified through thermal annealing in the presence of crustal fluids at about 1.5 Ga (ref. [14]). Together, these meteorites provide means of assessing the H-isotopic composition of water in the Martian crust at two endpoints separated by ~2.4 Gyr. The mineral apatite ($Ca_5(PO_4)_3[OH,F,Cl]$) is the only hydrous mineral common to both samples; hence, it was used to assess the H_2O content and H-isotopic composition of the Martian crustal samples by nanoscale secondary ion mass spectrometry (Methods). Apatite grains within these samples display a similar spread in D/H ratios (between ~3.12×10^{-4} and 4.67×10^{-4}) over a wide range of water contents (Fig. 1). The data for both samples are in agreement with H-isotopic data on other lithic clasts in NWA7034 and its pair NWA7533[15,16] and intercumulus apatite in ALH84001[17]. Our results are also consistent with D/H values reported for the Martian crust within the time span of 0.7 to 472 million years ago (Ma) (D/H ratio ~3.12×10^{-4} to 5.73×10^{-4})[18] and analyses of Hesperian (~3 Ga) clays

[1]NASA Johnson Space Center, Houston, TX, USA. [2]Lunar and Planetary Laboratory, University of Arizona, Tucson, AZ, USA. [3]NASA Glenn Research Center, Cleveland, OH, USA. [4]Scripps Institution of Oceanography, La Jolla, CA, USA. [5]The Open University, Milton Keynes, UK. [6]Max-Planck-Institut für Chemie, Mainz, Germany. [7]MTA Atomki, Debrecen, Hungary. [8]The Natural History Museum, London, UK. [9]Institute of Meteoritics, Department of Earth and Planetary Sciences, University of New Mexico, Albuquerque, NM, USA. ✉e-mail: jjbarnes@lpl.arizona.edu

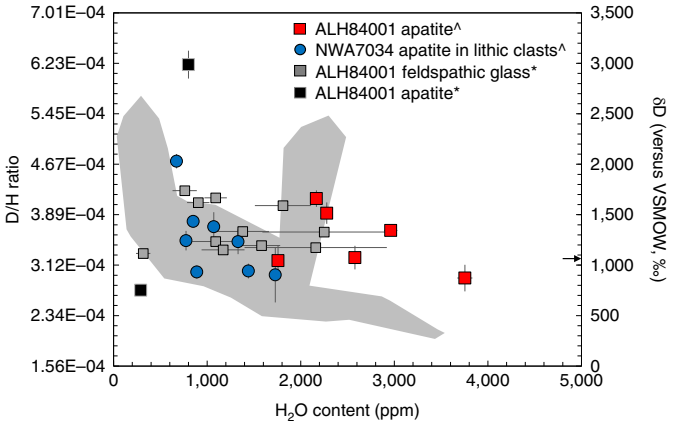

Fig. 1 | Hydrogen isotopic composition versus H_2O content of mineral phases in Martian crustal lithologies. Our new data demonstrate that both rocks sampled water of similar D/H ratio. Uncertainties are 2σ analytical error. Data sources: ^ refers to data from this study; * refers to compiled data for ALH84001 feldspathic glass from Leshin[28] and ALH84001 apatite from Boctor et al.[17]. The grey cloud is for NWA7034/7533 data from Hu et al.[16] and Liu et al.[15]. The arrow points towards a single high H_2O content value at 7,200 ppm in ALH84001[17].

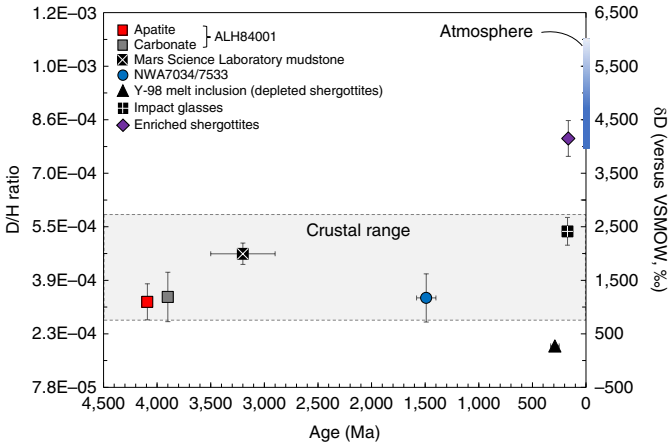

Fig. 2 | Age constraints on the hydrogen isotopic composition of the Martian crust. Despite the wide range in ages (Supplementary Information), different materials representing the Martian crust, including interactions with fluids, show similar D/H compositions. This crustal signature is distinct from the enriched shergottite source, the present-day atmosphere[2–4] and the light mantle defined by a subset of depleted shergottites[6,22,26]. Uncertainties are 1 s.d. about the mean. Any range in age (Supplementary Information) is smaller than the symbol size. Note that the enriched shergottite age is the average age of four samples (Grove Mountains 020090, Larkman Nunatak 06319, Los Angeles and Shergotty); for data and methods see Supplementary Information.

by the Sample Analysis at Mars (SAM) instrument on board the Mars Science Laboratory rover (D/H ratio of $(4.67 \pm 0.31) \times 10^{-4}$)[8]. Combined, these results indicate that the Martian crust is characterized by D/H ratios that are depleted in D relative to the current Martian atmosphere (Fig. 2) over a time span of at least the past 3.9 Gyr with a bulk crustal D/H ratio ranging from 2.68×10^{-4} to 5.73×10^{-4}.

The crust as the dominant water reservoir on Mars

The crust is the largest reservoir of water per unit mass on Mars, with an estimated H_2O abundance of 1,410 ppm (ref. [9]). This reservoir represents approximately 35% of the total budget of water on Mars, and our results indicate that this major water reservoir has had a fairly consistent H-isotopic composition since the first 660 Myr of Mars's history (Fig. 2). The Martian crust is composed of partial melting products of the Martian mantle that have erupted onto the surface or stalled within earlier-formed crust over the past 4.55 Gyr (refs. [19,20]), so the crust probably reflects geochemical signatures from the Martian mantle as well as any surficial hydrosphere/atmosphere at the time of emplacement. Consequently, the H-isotopic composition of the Martian crust reflects mixing of isotopically distinct mantle reservoirs, the amount of atmospheric loss of H that occurred within the first 660 Myr of Mars's history during the period Mars was thought to have a global magnetic field[21], or a combination thereof. To distinguish among these possible models, we have compiled and evaluated H-isotopic data from Martian meteorite samples that are thought to represent partial melts of the Martian mantle (Supplementary Information). In particular, we evaluated H-isotopic compositions relative to other geochemical indicators of mantle source character given that it has been long recognized that basalts from the Martian interior arise from at least two geochemically distinct mantle reservoirs, referred to as the depleted shergottite source and the enriched shergottite source. Moreover, a recent study has shown that there are differences in H_2O abundances between the enriched and depleted shergottite sources with the enriched source having 36–72 ppm H_2O and the depleted source having 14–23 ppm H_2O[9]. Details regarding other geochemical distinctions among these mantle reservoirs are provided in the Supplementary Information.

Distinguishing multiple mantle H reservoirs

Previous work converged on the idea that the Martian mantle has a lower D/H ratio than the atmosphere[6,22], although there has been some debate as to the most appropriate value of the mantle D/H ratio[6,23,24]. The most popular interpretation of a mantle signature[6,7,18] recorded in shergottites is a D/H ratio of ~1.99×10^{-4} from an olivine-hosted melt inclusion in the depleted olivine-phyric shergottite Yamato 980459[6]. Departures of H-isotopic compositions of phases within shergottites from this 'mantle' value are typically attributed to secondary processes such as contamination by fluids, shock implantation of D-rich modern atmosphere and/or contribution from terrestrial contamination[17,18,22–26].

When a holistic and texturally constrained view of the hydrogen isotopic compositions of shergottites is considered, the enriched shergottites are substantially more D-rich[7] (average D/H ratio of $(8.03 \pm 0.52) \times 10^{-4}$, see Methods) than the crust and within the range of reported values for the Martian atmosphere. By contrast, the depleted shergottites show much more variable intraphase and intrasample D/H ratios from 1.21×10^{-4} to $>8.57 \times 10^{-4}$ (Fig. 3a). We modelled the D/H variation observed in shergottites as if it were the result of simple two-component mixing between a D-poor mantle and a D-rich modern atmosphere (Methods), as suggested by previous studies[18,22–25]. The results imply that this process must have been more effective or selective in replacing hydrogen in enriched shergottites compared with depleted shergottites. The former require almost complete overprinting of initial D/H by the Martian atmosphere (Fig. 3a,b) within multiple phases that host a wide range of H_2O abundances and occur in a variety of textural regimes within the samples (Methods). In fact, the compiled D/H and shock pressure data reveal that shock implantation of hydrogen cannot account for the D/H systematics of the enriched shergottites (Extended Data Fig. 1), and this refutes shock-implanted atmospheric contamination as a sole explanation for the observed D/H variation in shergottites (Supplementary Information).

Although large intrasample variation in D/H is observed for depleted and enriched shergottites as well as other Martian

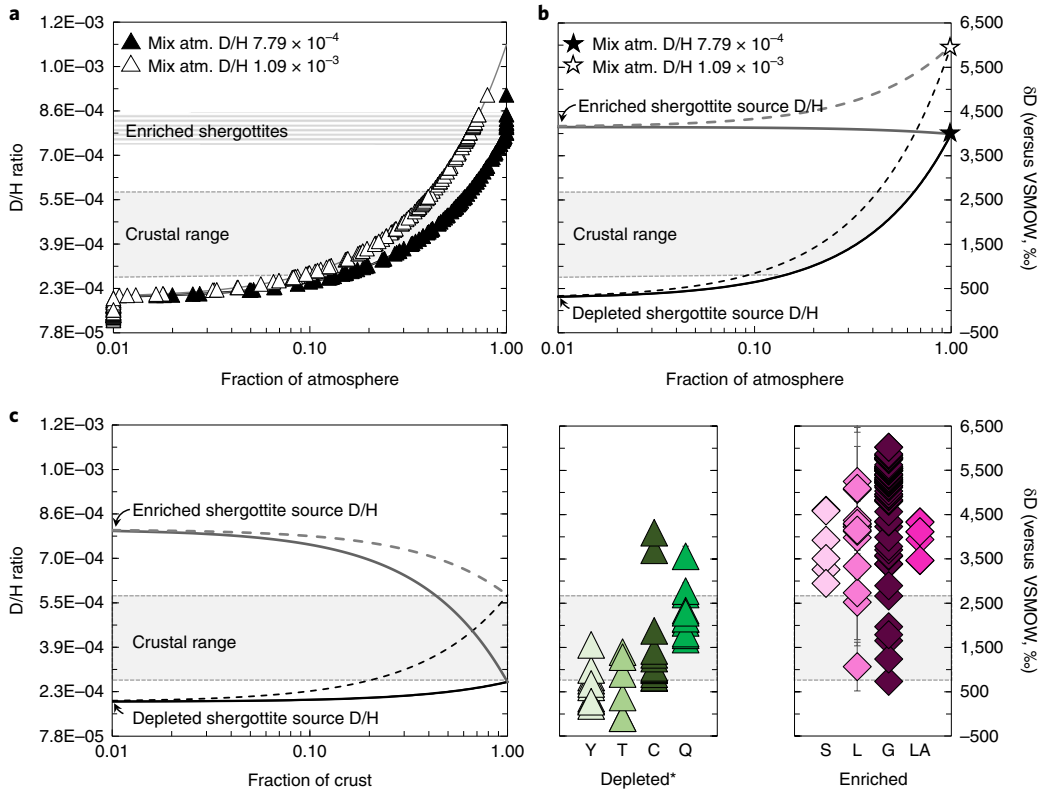

Fig. 3 | Mixing models and texturally constrained observations used to define multiple mantle H reservoirs. The mixing calculations simulate the atomic replacement of hydrogen in Martian basalts by the Martian atmosphere. We assumed that when the Martian mantle partially melted to produce shergottites, the partial melts retained the D/H of their respective mantle source regions (Methods). **a**, The mixing curves between the depleted shergottite-like D/H and the atmosphere. Plotted along the curves are the D/H data for the depleted shergottites (Methods). The *x* axis shows the fraction of atmospheric D/H needed to explain the observed D/H ratios. The D/H of the atmosphere was varied on the basis of two endpoints[2–4]. **b**, The mixing of both enriched and depleted shergottite mantle values with the atmosphere defined for two endpoint D/H ratios[2–4]. **c**, The mixing lines between the low D/H depleted shergottite mantle with crustal H_2O and high D/H enriched shergottite mantle with crustal H_2O. Also plotted in **c** are the values and 2σ analytical errors for samples derived from geochemically depleted sources (* denotes Y-98 (Y), Tissint (T), Chassignites (C), QUE94201 (Q)) and enriched shergottites (Shergotty (S), Larkman Nunatak 06319 (L), Grove Mountains 020090 (G), Los Angeles (LA)). Both groups of samples show evidence of mixing between mantle and crustal water.

meteorites such as the chassignites, many samples exhibit limited ranges in D/H that do not span the full range of values between the canonical light mantle and heavy atmosphere. Consequently, we also evaluated the D/H data in Martian meteorites in the context of mixing between a mantle source and the Martian crust (Fig. 3c). The variation in D/H of enriched shergottites extends between a lower D/H endmember that is within the range we define for the Martian crust and a high D/H endmember we infer to be representative of their mantle source. The depleted shergottites and chassignites, which originate from geochemically depleted portions of the Martian mantle, exhibit at least two types of intrasample D/H variation. One type is best represented by the olivine-phyric shergottites Yamato 980459 and Tissint, which exhibit variation in D/H that extend between a high D/H endmember that is within the range we define for the Martian crust and a low D/H endmember that we and previous studies have inferred to be representative of their mantle source (Fig. 3c). The second type is best represented by chassignites and Queen Alexandra Range (QUE) 94201, which exhibit variation in D/H that extend between a low D/H endmember that is within the range we define for the Martian crust and a high D/H endmember that we infer to be representative of their mantle source[17,23,27,28] (Fig. 3c). Importantly, the geochemistry of Chassigny refutes an atmospheric component[29,30], although it may have exchanged with crustal H_2O[31,32], and the bulk composition of QUE94201 refutes substantial crustal assimilation[33,34], so the source of the elevated D/H may not be from the Martian crust (see Methods). These observations indicate the geochemically depleted mantle source(s) is heterogeneous with respect to D/H ratio and raise the possibility that heavy hydrogen was redistributed within the mantle from the relatively wet enriched shergottite source to the relatively drier depleted sources[9] by mantle metasomatism.

The H-isotope data for Martian meteorites clearly indicate that the Martian mantle has at least two isotopically distinct mantle reservoirs, with one mantle reservoir characterized by a D/H ratio of $\sim 1.99 \pm 0.02 \times 10^{-4}$ that is associated with a subset of geochemically depleted Martian basalts and the other source characterized by a D/H of at least $(8.03 \pm 0.52) \times 10^{-4}$ that is associated with the geochemically enriched Martian basalts. This model rejects the paradigm of a single H-isotopic reservoir in the Martian mantle[6,7], and it relaxes previous requirements of pervasive atmospheric contamination of all the enriched shergottites (Fig. 3b), although atmospheric contamination is certainly an explanation for elevated D/H ratios in some samples[24,25].

Formation of a geochemically heterogeneous mantle

The existence of at least two distinct H-isotopic reservoirs within the Martian mantle indicates that the H-isotopic composition of the Martian crust represents, at minimum, a mixture of two mantle reservoirs and may also represent a third component defined by the primordial atmosphere/hydrosphere within the first 660 Myr

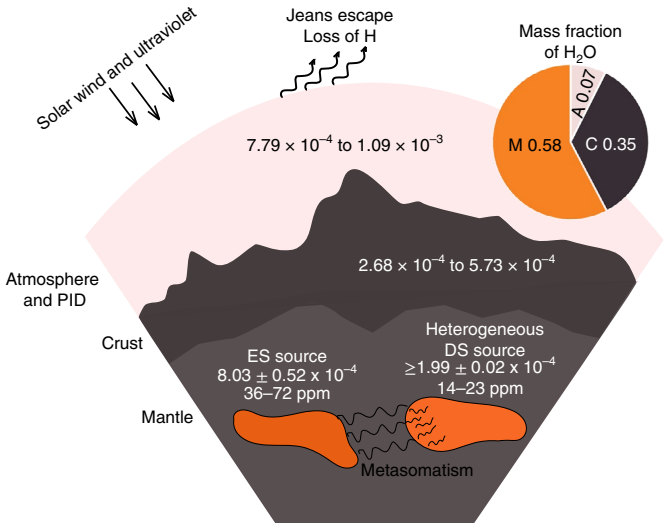

Fig. 4 | Illustration showing the present-day hydrogen reservoirs in and on Mars. The mass fractions (pie chart) of Martian H_2O are based on the mass of H_2O in the bulk crust (C), the mantle (M) and the combined inventory (A) of the atmosphere and polar ice deposits (PID)[3,9]. The mantle mass fraction is the combination of depleted shergottites (DS) and enriched shergottites (ES). For data sources, see Methods.

of Mars's history (Fig. 4), although pristine crustal samples that are older than 3.9 Ga are needed to characterize the D/H ratio of the primordial surface hydrosphere/atmosphere of Mars. The presence of at least two isotopically distinct H-isotopic reservoirs in the Martian mantle has important implications for the differentiation and subsequent thermochemical evolution of Mars. The ages of the depleted and enriched shergottite sources indicate that they are both primordial features of the Martian interior[35,36]. Previous models have called upon multiple episodes of melting in the primordial Martian mantle to account for the geochemical differences in source character between the depleted and enriched shergottites[35,37]. However, melting processes at pressure cannot account for the stark differences in H-isotopic composition between the depleted and enriched sources. Consequently, these features may have been inherited from the primary building blocks that constructed Mars[38–40], implying that the Martian mantle has almost always been heterogeneous because it was poorly mixed during accretion, differentiation and its subsequent thermochemical evolution (Supplementary Information). These results call into question the canonical model of differentiation on Mars via a globally extensive magma ocean, which would have worked to homogenize H-isotopic and other geochemical differences among disparate planetary building blocks. Additional studies are needed to further evaluate the efficacy of a globally extensive magma ocean on Mars, but the preservation of two distinct H-isotopic reservoirs in the Martian mantle is an important new paradigm for any model to describe the formation, differentiation and physicochemical evolution of Mars[39,41].

Online content

Any methods, additional references, Nature Research reporting summaries, source data, extended data, supplementary information, acknowledgements, peer review information; details of author contributions and competing interests; and statements of data and code availability are available at https://doi.org/10.1038/s41561-020-0552-y.

Received: 17 June 2019; Accepted: 10 February 2020;
Published online: 30 March 2020

References

1. Filiberto, J. & Schwenzer, S. P. *Volatiles in the Martian Crust* (Elsevier, 2018).
2. Villanueva, G. L. et al. Strong water isotopic anomalies in the Martian atmosphere: probing current and ancient reservoirs. *Science* **348**, 218–221 (2015).
3. Krasnopolsky, V. A. Variations of the HDO/H_2O ratio in the Martian atmosphere and loss of water from Mars. *Icarus* **257**, 377–386 (2015).
4. Bjoraker, G. L., Mumma, M. J. & Larsen, H. P. Isotopic abundance ratios for hydrogen and oxygen in the Martian atmosphere. *Bull. Am. Astron. Soc.* **21**, 991 (1989).
5. Chassefière, E. & Leblanc, F. Mars atmospheric escape and evolution; interaction with the solar wind. *Planet. Space Sci.* **52**, 1039–1058 (2004).
6. Usui, T., Alexander, C. M. O. D., Wang, J., Simon, J. I. & Jones, J. H. Origin of water and mantle–crust interactions on Mars inferred from hydrogen isotopes and volatile element abundances of olivine-hosted melt inclusions of primitive shergottites. *Earth Planet. Sci. Lett.* **357–358**, 119–129 (2012).
7. Hallis, L. J. D/H ratios of the inner Solar System. *Philos. Trans. R. Soc. A* **375**, 20150390 (2017).
8. Mahaffy, P. R. et al. The imprint of atmospheric evolution in the D/H of Hesperian clay minerals on Mars. *Science* **347**, 412–414 (2014).
9. McCubbin, F. M. et al. Heterogeneous distribution of H_2O in the Martian interior: implications for the abundance of H_2O in depleted and enriched mantle sources. *Meteorit. Planet. Sci.* **51**, 2036–2060 (2016).
10. Lapen, T. J. et al. A younger age for ALH84001 and its geochemical link to shergottite sources in Mars. *Science* **328**, 347–351 (2010).
11. Terada, K., Monde, T. & Sano, Y. Ion microprobe U-Th-Pb dating of phosphates in Martian meteorite ALH 84001. *Meteorit. Planet. Sci.* **38**, 1697–1703 (2003).
12. Borg, L. E. et al. The age of the carbonates in Martian meteorite ALH84001. *Science* **286**, 90–94 (1999).
13. Agee, C. B. et al. Unique meteorite from early Amazonian Mars: water-rich basaltic breccia Northwest Africa 7034. *Science* **339**, 780–785 (2013).
14. McCubbin, F. M. et al. Geologic history of Martian regolith breccia Northwest Africa 7034: evidence for hydrothermal activity and lithologic diversity in the Martian crust. *J. Geophys. Res. Planets* **121**, 2120–2149 (2016).
15. Liu, Y., Ma, C., Beckett, J. R., Chen, Y. & Guan, Y. Rare-earth-element minerals in Martian breccia meteorites NWA 7034 and 7533: implications for fluid–rock interaction in the Martian crust. *Earth Planet. Sci. Lett.* **451**, 251–262 (2016).
16. Hu, S. et al. Ancient geologic events on Mars revealed by zircons and apatites from the Martian regolith breccia NWA 7034. *Meteorit. Planet. Sci.* **879**, 850–879 (2019).
17. Boctor, N. Z., Alexander, C. M. O. D., Wang, J. & Hauri, E. H. The sources of water in Martian meteorites: clues from hydrogen isotopes. *Geochim. Cosmochim. Acta* **67**, 397–3989 (2003).
18. Usui, T., Alexander, C. M. O. D., Wang, J., Simon, J. I. & Jones, J. H. Meteoritic evidence for a previously unrecognized hydrogen reservoir on Mars. *Earth Planet. Sci. Lett.* **410**, 140–151 (2015).
19. Borg, L. & Drake, M. J. A review of meteorite evidence for the timing of magmatism and of surface or near-surface liquid water on Mars. *J. Geophys. Res. Planets* **110**, E12S03 (2005).
20. Bouvier, L. C. et al. Evidence for extremely rapid magma ocean crystallization and crust formation on Mars. *Nature* **558**, 586–589 (2018).
21. Lillis, R. J., Frey, H. V. & Manga, M. Rapid decrease in Martian crustal magnetization in the Noachian era: implications for the dynamo and climate of early Mars. *Geophys. Res. Lett.* **35**, 2–7 (2008).
22. Hallis, L. J. et al. Effects of shock and Martian alteration on Tissint hydrogen isotope ratios and water content. *Geochim. Cosmochim. Acta* **200**, 280–294 (2017).
23. Watson, L., Hutcheon, I. D., Epstein, S. & Stolper, E. M. Water on Mars: clues from deuterium/hydrogen and water contents of hydrous phases in SNC meteorites. *Science* **265**, 86–90 (1994).
24. Greenwood, J. P., Itoh, S., Sakamoto, N., Vicenzi, E. P. & Yurimoto, H. Hydrogen isotope evidence for loss of water from Mars through time. *Geophys. Res. Lett.* **35**, L05203 (2008).
25. Liu, Y. et al. Impact-melt hygrometer for Mars: the case of shergottite Elephant Moraine (EETA) 79001. *Earth Planet. Sci. Lett.* **490**, 206–215 (2018).
26. Mane, P. et al. Hydrogen isotopic composition of the Martian mantle inferred from the newest Martian meteorite fall, Tissint. *Meteorit. Planet. Sci.* **51**, 2073–2091 (2016).
27. Giesting, P. A. et al. Igneous and shock processes affecting chassignite amphibole evaluated using chlorine/water partitioning and hydrogen isotopes. *Meteorit. Planet. Sci.* **50**, 433–460 (2015).
28. Leshin, L. A. Insights into Martian water reservoirs from analyses of Martian meteorite QUE94201. *Geophys. Res. Lett.* **27**, 321–333 (2000).
29. Mathew, K. J. & Marti, K. Early evolution of Martian volatiles: nitrogen and noble gas components in ALH84001 and Chassigny. *J. Geophys. Res. Planets* **106**, 1401–1422 (2001).

30. Ott, U. Noble gases in SNC meteorites: Shergotty, Nakhla, Chassigny. *Geochim. Cosmochim. Acta* **52**, 1937–1948 (1988).
31. McCubbin, F. M. et al. A petrogenetic model for the comagmatic origin of chassignites and nakhlites: inferences from chlorine-rich minerals, petrology, and geochemistry. *Meteorit. Planet. Sci.* **48**, 819–853 (2013).
32. McCubbin, F. M. & Nekvasil, H. Maskelynite-hosted apatite in the Chassigny meteorite: insights into late-stage magmatic volatile evolution in Martian magmas. *Am. Mineral.* **93**, 676–684 (2008).
33. Williams, J. T. et al. The chlorine isotopic composition of Martian meteorites 1: chlorine isotope composition of Martian mantle and crustal reservoirs and their interactions. *Meteorit. Planet. Sci.* **51**, 2092–2110 (2016).
34. Franz, H. et al. Isotopic links between atmospheric chemistry and the deep sulphur cycle on Mars. *Nature* **508**, 364–368 (2014).
35. Borg, L. E., Nyquist, L. E., Taylor, L. A., Wiesmann, H. & Shih, C. Y. Constraints on Martian differentiation processes from Rb-Sr and Sm-Nd isotopic analyses of the basaltic shergottite QUE 94201. *Geochim. Cosmochim. Acta* **61**, 4915–4931 (1997).
36. Borg, L. E., Nyquist, L. E., Wiesmann, H., Shih, C. Y. & Reese, Y. The age of Dar al Gani 476 and the differentation history of the Martian meteorites inferred from their radiogenic isotopic systematics. *Geochim. Cosmochim. Acta* **67**, 3519–3536 (2003).
37. Herd, C. D. K. The oxygen fugacity of olivine-phyric Martian basalts and the components within the mantle and crust of Mars. *Meteorit. Planet. Sci.* **38**, 1793–1805 (2003).
38. Chambers, J. E. Planetary accretion in the inner Solar System. *Earth Planet. Sci. Lett.* **223**, 241–252 (2004).
39. Dauphas, N. & Pourmand, A. Hf-W-Th evidence for rapid growth of Mars and its status as a planetary embryo. *Nature* **473**, 489–492 (2011).
40. McCubbin, F. M. & Barnes, J. J. Origin and abundances of H_2O in the terrestrial planets, Moon, and asteroids. *Earth Planet. Sci. Lett.* **526**, 115771 (2019).
41. Tang, H. & Dauphas, N. 60Fe-60Ni chronology of core formation in Mars. *Earth Planet. Sci. Lett.* **390**, 264–274 (2014).

Methods

Scanning electron microscope analysis. Two standard polished thin sections of NWA7034 (Institute of Meteoritics (IOM) numbers: 1B,2 and 2,3) were analysed as well as two thin sections of ALH84001 (thin section numbers: 7 and 205). Thin sections of NWA7034 were characterized for a previous study by Santos et al.[44]. Detailed imaging of the target grains for this study were made using a Quanta three-dimensional focused ion beam scanning electron microscope at the Open University (OU), Milton Keynes, fitted with an Oxford Instruments INCA energy-dispersive X-ray detector. Thin sections were coated with carbon and analytical conditions followed those used in previous studies (for example, Barnes et al.[45]). Thin sections of ALH84001 were characterized using the JEOL 7600F scanning electron microscope at NASA's (National Aeronautics and Space Administration's) Johnson Space Center (JSC) in Houston. Each thin section was carbon coated with ~15 nm of carbon and X-ray mapped using an accelerated electron beam of 15 kV and 1.5 nA.

Back-scattered electron and secondary electron images of the phosphates analysed by NanoSIMS from NWA7034 and ALH84001 are provided in the Supplementary Information. For NWA7034, clast numbers and lithologies were previously described by Santos et al.[44]. Clasts analysed in NWA7034 include iron, titanium and phosphorous-rich clasts (#2, #64), basaltic clasts (#3, #5, #75) and a trachyandesite clast (#76).

Electron probe microanalysis. Chemical analyses of apatites in lithic clasts in NWA7034 have already been reported by McCubbin et al.[9], and those data were utilized in this study (see Supplementary Information). Electron probe microanalysis was performed on apatites in thin sections of ALH84001 using the JEOL 8530F at JSC. Data were collected using both the JEOL manufacturer's software and the Probe for EPMA software from Probe Software. All apatites were analysed using a 15 kV accelerating voltage and 20 nA beam current following previous procedures established by our group for the analysis of apatite in planetary materials[44,45]. We analysed the elements Si, Fe, Mg, Mn, Ca, Na, P, Al, Y, Ce, F and Cl in each apatite. Fluorine was analysed using a light-element artificial layered dispersive element (LDE1) detector crystal, and Cl was analysed using a pentaerythritol (PETL) detector crystal. The standards were as follows: for Ca, a Durango apatite[46] was used as the primary standard, for P, SPI Supplies apatite was used as the primary standard, and a natural fluorapatite from India (Ap020) from McCubbin et al.[47] was used as a secondary check on the standardization. A synthetic SrF_2 crystal from the Taylor multi-element standard mount (C. M. Taylor) was used as the primary F standard, and Ap020 was used as an additional check on the F standardization. A tugtupite crystal was used as a primary Cl standard. Rhodonite, albite, diopside and olivine from the Taylor multi-element standard mount (C. M. Taylor) were used as a primary standard for Mn, Na, Si and Mg, respectively. Ilmenite from the Smithsonian (USNM 133868) was used as a primary standard for Fe. Cerium and Y were standardized using their respective synthetic orthophosphate endmembers from Jarosewich and Boatner[48]. To reduce or eliminate electron beam damage, we used a 5 µm spot for standardization and 1–5 µm diameter beams for analysis of apatite grains in the Martian samples.

After analysis by electron microbeam techniques, the carbon coatings were removed from the thin sections using a clean soft polishing pad and isopropanol alcohol. The samples were all cleaned in isopropanol alcohol in an ultra-sonication bath and stored in a vacuum oven at ~60 °C until they were gold coated for seconday ion mass spectrometer (SIMS) analysis.

Ion probe microanalysis. The CAMECA nanoscale secondary ion mass spectrometer (NanoSIMS) 50L ion probes at (1) The OU and (2) JSC were used in this work. Analyses followed similar protocols to those detailed in previous studies (for example, refs. [45,49,50]). Specifically, NWA7034 was analysed using the OU NanoSIMS, and ALH84001 was analysed using the NanoSIMS at JSC. Note that here and in the figures we present H-isotopic compositions using standard delta notation, where $\delta D = ((D/H_{sample}/D/H_{VSMOW}) - 1) \times 1{,}000$, where VSMOW is Vienna Standard Mean Ocean Water with a D/H ratio of 1.557×10^{-4}. Details of assessment of background H are provided in the Supplementary Information.

Technical protocol. Thin sections were gold coated before ion probe analysis; ~30 nm Au was used at the OU and ~10 nm Au was used at JSC.

1. The OU NanoSIMS was operated in multi-collection mode over two analytical sessions in 2015. A large Cs^+ primary beam of ~300 pA was rastered on the sample surface over an ~12 µm × 12 µm area during pre-sputtering (to eliminate surface contamination) and over an ~5 µm × 5 µm area during analysis. For the analysis, secondary ions of ^1H, ^2H, ^{13}C and ^{18}O were collected simultaneously from the central 6.25 µm² area of each raster area on electron multipliers for ~20 min. An electron flood gun was used for additional charge compensation and tuned to minimize its contribution to the background. The mass resolving power was set to ~4,000.
2. The JSC NanoSIMS was operated in multi-collection mode. A large Cs^+ primary beam of ~700pA current was rastered on the sample surface over a 20 µm × 20 µm area during an ~5 min pre-sputter to eliminate any remaining surface contamination. For the analysis, areas of ~10 µm × 10 µm were rastered, and signal was collected from central regions of between ~19 and 25 µm², negative secondary ions of ^1H, ^2H, ^{13}C and ^{18}O were collected simultaneously on electron multipliers during the ~15 min analysis. An electron flood gun was used for additional charge compensation and tuned to minimize its contribution to the background. The mass resolving power was set to ~4,000.

Calibration and error analysis.

1. Reference apatites were used for calibrating water contents in unknowns and for establishing and correcting for instrumental mass fractionation. These standards included Ap018 (~0.2 wt% H_2O), Ap003 (~0.06 wt.% H_2O) and Ap004 (~0.55 wt.% H_2O) (details in McCubbin et al.[47]). The 2σ uncertainty on the calibration slope varied between 2 and 3% over the two sessions. Reference apatite Ap004 was used to correct measured D/H ratios for instrumental mass fractionation in both sessions. The reproducibility of the D/H ratios measured on the reference apatites varied from 8‰ to 40‰ (2σ) in session 1 and from 28‰ to 52‰ (2σ) in session 2. For unknowns, the H_2O contents and D/H ratios, given using standard delta (δ) notation with respect to the D/H ratio of the VSMOW, and corrected for instrumental mass fractionation on the basis of repeated measurements of reference apatites, are reported with their 2σ uncertainties derived from the reproducibility of associated blocks of standard analyses (usually four analyses per block) and the internal precision of each analysis.
2. The reference apatites used at JSC (different crystals mounted in indium) included Ap018 (~0.2 wt% H_2O), Ap003 (~0.06 wt.% H_2O) and Ap005 (~0.37 wt.% H_2O)[47]. The 2σ uncertainty on the calibration slope was ~4% during the analytical session. Reference apatite Ap018 was used to correct measured D/H ratios for instrumental mass fractionation. The reproducibility of the D/H ratios measured on the reference apatites varied from 16‰ to 28‰ (2σ s.d.).

Secondary ion images of ^1H and ^{13}C were monitored during pre-sputtering to further ensure that the analysed areas were free of any surficial contamination, cracks or hotspots. Unfortunately, hidden cracks often appeared during analysis of apatites in the Martian rocks. In such cases, only portions of the secondary ion signal corresponding to analysis of pristine material were considered, and further processing was performed using the NanoSIMS DataEditor software developed by F. Gyngard while at Washington University St Louis. Data inclusion was based on the ^{13}C signal, which is low in Martian apatites but is several orders of magnitude higher for crack-filling material. This technique has been validated previously[49].

The data obtained in this study are provided in Supplementary Table 1 and are plotted in Fig. 1. The apatites analysed are shown in Supplementary Figs. 3–9.

Computing isotopically distinct reservoirs. The geochemically depleted shergottites display a large range in δD values from ~−222 to 4,867‰ (ref. [7] and Supplementary Information). In this study, the average D/H ratio of each sample was used to define a weighted average to avoid bias from well-studied samples. The weighted average δD value of depleted shergottites is 1,369 ± 632‰ (Supplementary Information) (s.d., $n = 157$, $n_{samples} = 5$ (refs. [6,17,18,22,26,28,51,52])). However, there are large ranges within individual melt inclusions, feldspathic glass inclusions, phosphates and olivine. The large range in D/H of the depleted shergottites, on the surface, looks to be consistent with previous models proposing mixing between a light mantle reservoir and a heavy atmospheric reservoir (Fig. 3a); however, when the ranges of D/H ratios for individual samples of depleted shergottites are compared, many samples exhibit limited ranges that would be more consistent with crustal assimilation (Fig. 3c), although some samples do exhibit the entire range of values.

Yamato 980459 (Y-98) has been one of the defining samples for understanding the geochemical nature of the depleted shergottite source[6,53–58], and Usui et al.[6] reported a light D/H value for an olivine-hosted melt inclusion for Y-98. Furthermore, groundmass glasses in Y-98 exhibit a range of δD values[18] between 181 and 1,562‰ (Fig. 3c). In addition, melt inclusions in the depleted shergottite Tissint, which was a fall and hence has had limited uncontrolled exposure to the terrestrial weathering environment, exhibits a range of D/H ratios[22,26] that are similar to melt inclusion and groundmass glass data[6,18] from Y-98 (Fig. 3c). Consequently, we used the D/H ratio[6] of an olivine-hosted melt inclusion in Y-98 to represent an upper limit on the depleted mantle D/H, which overlaps with some Tissint olivine-hosted melt inclusions[22,26] and other values commonly considered 'Martian mantle'[6,7,18,59]. The ranges of D/H values of Tissint and Y-98 span between a light mantle source and the range of values we present for the Martian crust (Fig. 3c), although we cannot rule out mixing between a light mantle source and small amounts of atmosphere. It is important to note that some samples from depleted sources have elevated D/H ratios[40] that cannot be attributed to having come from a mantle source with low D/H ratios. The ranges in D/H values of QUE94201 and Chassignites[17,23,27,28] span between a high D/H endmember and the range of values we present for the Martian crust (Fig. 3c). On the basis of other geochemical indicators, these high D/H ratios are inconsistent with mixing of either crustal[8,33] or atmospheric[29,30] D/H, respectively. Data from QUE94201 indicate the presence of a heavy hydrogen component in depleted

Martian mantle, whereas data for Chassignites could represent mixing between such a heavy component and crustal water (Fig. 3c). The enriched shergottites also span a large range of values from −204 to 6,830‰; however, most of the in situ measurements of minerals (excluding nominally anhydrous minerals) and melt inclusions in the geochemically enriched Martian shergottites yield a range in δD values from ~512 to 6,830‰ and a weighted average of 3,876 ± 730‰ (s.d., $n = 99$, $n_{samples} = 5$ (refs. [6,23,24,59–61])). If we consider petrographic and textural constraints, and core–rim variations, a more appropriate value of 4,158 ± 336‰ is obtained (s.d., $n = 22$, $n_{samples} = 4$ (refs. [6,24,60,61])). These values overlap and provide confidence that the enriched shergottite source is isotopically distinct from that of the depleted shergottites. We used the weighted average value of 4,158 ± 336‰ in our calculations, but we note that the δD value of the enriched shergottite mantle source is probably higher than this value.

A compilation of literature data used in this study can be found in Supplementary Table 2. It includes H isotope data previously published for NWA7034 (and paired samples) and ALH84001. We also compiled in situ H isotope data for enriched and depleted shergottites, as well as other geochemical information relevant to the discussion portion of this work.

Mass balance calculations. The relative mass of water in each Martian reservoir was calculated for use in subsequent mixing models. For this task, the water contents in each reservoir determined by McCubbin et al.[9] were used. Those values are ~1,410 ppm H_2O in the crust, 36–72 ppm H_2O in the enriched shergottite source and 14–23 ppm H_2O in the depleted shergottite source. In addition to these reservoirs, there is the surface atmosphere/hydrosphere that includes ~100 ppm H_2O in the present-day Martian atmosphere[3] and the present-day polar ice deposits, which are estimated to constitute a global layer on the Martian surface of 34 m in thickness[62]. On the basis of these values, the mass of water in the crust, exclusive of the atmosphere and surface hydrosphere, is estimated to be ~2.33×10^{19} kg H_2O (see McCubbin et al.[9]), and the mass of water in the Martian atmosphere/surface cryosphere is estimated to be 4.91×10^{18} kg H_2O[3,9,62]. We cannot differentiate the relative amounts of water between the enriched and depleted shergottite mantle sources with respect to the entire mantle as we do not know the relative size/distribution of each source. However, McCubbin et al.[9] estimated that the bulk silicate Mars has 137 ppm H_2O, which, when we subtract the contributions from the crust and from the atmosphere and surface polar ices, means there is ~3.84×10^{19} kg H_2O in the mantle (computed from McCubbin et al.[9]). This allows us to compute the relative mass fractions of water hosted in the atmosphere/hydrosphere, crust and mantle to be 0.07, 0.35 0.58, respectively (Fig. 4).

Hydrogen isotope mixing models. Binary (linear) mixing calculations were performed to simulate the atomic replacement of hydrogen in Martian basalts by Martian atmosphere (Fig. 3). These are not constrained by mass balance of water (see the following). These calculations were used simply to show how much atmospheric replacement of hydrated components would be required in Martian basalts to explain the data observed in chemically distinct shergottites. We assumed that when Martian shergottites partially melted, they retained the original D/H of their source, that is, 1.99×10^{-4} (from Usui et al.[6]) and 8.03×10^{-4} (see the preceding) for the depleted and enriched shergottite sources, respectively. The atmosphere[2–4] was assumed to have a D/H of either 7.79×10^{-4} or 1.09×10^{-3}. Complete replacement of mantle D/H was achieved when the fraction of atmosphere reached a value of 1. Figure 3a shows the mixing of water between depleted shergottites and the atmosphere, which is the previously proposed model to explain variations in D/H of Martian samples[18,22–25]. Plotted along the line are all of the data available for depleted shergottites (Supplementary Information). The curve was used to calculate the fraction of atmospheric D/H (or percentage replacement) needed to explain the departure of the observed D/H data from a source with low D/H (7.79×10^{-4}). Note that some depleted shergottite data cannot be explained by atmospheric replacement as modelled here (that is, those data that have lower D/H than Y-98 melt inclusion).

When the enriched shergottites are considered, the results show that if a Yamato 980459-like D/H is assumed for their source, then almost complete replacement of mantle-like D/H is required for a majority of enriched shergottite samples to reproduce the measured D/H values (Fig. 3). Specifically, when the atmospheric value is 7.79×10^{-4} using the curve in Fig. 3a, ~70% of the data for enriched shergottites require more than half of the initial D/H (that is, at 0.5 fraction) to be replaced by that of the atmosphere, compared with only 35% for the depleted shergottites. The crust lies between ~0.1 and 0.6 of the fraction of the atmosphere.

When mixing of a heavy enriched shergottite source is also considered (Fig. 3b), there is little difference in the resultant D/H with atmospheric mixing for the enriched shergottite samples unless the atmosphere has an extremely high D/H ratio (dashed line). This suggests that either the enriched shergottites have seen preferential replacement of D/H by the atmosphere compared with the depleted shergottites or the source for the enriched shergottites was already heavy before any mixing. Notably, if the enriched shergottite source does indeed have a distinct D/H, variations in the D/H among the shergottites (outside of textural or chemical evidence for atmospheric interaction) could be the result of D/H mixing between the two mantle sources and/or the crust (Fig. 3b).

We also performed mass balance-constrained isotopic mixing models (Supplementary Fig. 1), and details can be found in the Supplementary Information.

Data availability

All data generated or analysed during this study are included in this article and its supplementary information files. All new data associated with this paper will be made publicly available via The UA Campus Repository (https://repository.arizona.edu/).

References

42. Fritz, J., Artemieva, N. & Greshake, A. Ejection of Martian meteorites. *Meteorit. Planet. Sci.* **40**, 1393–1411 (2005).
43. Baziotis, I. P. et al. The Tissint Martian meteorite as evidence for the largest impact excavation. *Nat. Commun.* **4**, 1404 (2013).
44. Santos, A. R. et al. Petrology of igneous clasts in Northwest Africa 7034: implications for the petrologic diversity of the Martian crust. *Geochim. Cosmochim. Acta* **157**, 56–85 (2015).
45. Barnes, J. J. et al. The origin of water in the primitive Moon as revealed by the lunar highlands samples. *Earth Planet. Sci. Lett.* **390**, 244–252 (2014).
46. Jarosewich, E., Nelen, J. A. & Norbers, J. A. Reference samples for electron microprobe analysis. *Geostandard. Newslett.* **4**, 68–72 (1980).
47. McCubbin, F. M. et al. Hydrous melting of the Martian mantle produced both depleted and enriched shergottites. *Geology* **40**, 683–686 (2012).
48. Jarosewich, E. & Boatner, L. A. Rare earth element reference samples for electron microprobe analysis. *Geostandard. Newslett.* **15**, 397–399 (1991).
49. Tartèse, R. et al. The abundance, distribution, and isotopic composition of hydrogen in the Moon as revealed by basaltic lunar samples: implications for the volatile inventory of the Moon. *Geochim. Cosmochim. Acta* **122**, 58–74 (2013).
50. Barnes, J. J. et al. Accurate and precise measurements of the D/H ratio and hydroxyl content in lunar apatites using NanoSIMS. *Chem. Geol.* **337–338**, 48–55 (2013).
51. Chen, Y. et al. Evidence in Tissint for recent subsurface water on Mars. *Earth Planet. Sci. Lett.* **425**, 55–63 (2015).
52. Kuchka, C. R., Herd, C. D. K., Walton, E. L., Guan, Y. & Liu, Y. Martian low-temperature alteration materials in shock-melt pockets in Tissint: constraints on their preservation in shergottite meteorites. *Geochim. Cosmochim. Acta* **210**, 228–246 (2017).
53. Basu Sarbadhikari, A., Day, J. M. D., Liu, Y., Rumble, D. & Taylor, L. A. Petrogenesis of olivine-phyric shergottite Larkman Nunatak 06319: implications for enriched components in Martian basalts. *Geochim. Cosmochim. Acta* **73**, 2190–2214 (2009).
54. White, D. S. M., Dalton, H. A., Kiefer, W. S. & Treiman, A. H. Experimental petrology of the basaltic shergottite Yamato-980459: implications for the thermal structure of the Martian mantle. *Meteorit. Planet. Sci.* **41**, 1271–1290 (2006).
55. Usui, T., McSween, H. Y. & Floss, C. Petrogenesis of olivine-phyric shergottite Yamato 980459, revisited. *Geochim. Cosmochim. Acta* **72**, 1711–1730 (2008).
56. Symes, S. J. K., Borg, L. E., Shearer, C. K. & Irving, A. J. The age of the Martian meteorite Northwest Africa 1195 and the differentiation history of the shergottites. *Geochim. Cosmochim. Acta* **72**, 1696–1710 (2008).
57. Shearer, C. K. et al. Petrogenetic linkages among fO_2, isotopic enrichments-depletions and crystallization history in Martian basalts. Evidence from the distribution of phosphorus in olivine megacrysts. *Geochim. Cosmochim. Acta* **120**, 17–38 (2013).
58. Peters, T. J. et al. Tracking the source of the enriched Martian meteorites in olivine-hosted melt inclusions of two depleted shergottites, Yamato 980459 and Tissint. *Earth Planet. Sci. Lett.* **418**, 91–102 (2015).
59. Hallis, L. J. et al. Hydrogen isotope analyses of alteration phases in the nakhlite Martian meteorites. *Geochim. Cosmochim. Acta* **97**, 105–119 (2012).
60. Hu, S. et al. NanoSIMS analyses of apatite and melt inclusions in the GRV 020090 Martian meteorite: hydrogen isotope evidence for recent past underground hydrothermal activity on Mars. *Geochim. Cosmochim. Acta* **140**, 321–333 (2014).
61. Koike, M. et al. Combined investigation of hisotopic compositions and U-Pb chronology of young Martian meteorite Larkman Nunatak 06319. *Geochem. J.* **50**, 363–377 (2016).
62. Carr, M. H. & Head, J. W. Martian surface/near-surface water inventory: sources, sinks, and changes with time. *Geophys. Res. Lett.* **42**, 726–732 (2015).

Acknowledgements

This work was supported by the UK Science and Technology Facilities Council (grant no. ST/L000776/1 to M.A. and I.A.F.). J.J.B. thanks the NASA Postdoctoral Program for the fellowship under which part of the data collection and all the manuscript writing was performed. F.M.M. was supported by NASA's Planetary Science Research Program. We thank the Meteorite Working Group and the curation office at NASA Johnson Space Center (JSC) for allocation of Antarctic meteorite ALH84001,7 and 205.

The US Antarctic meteorite samples are recovered by the Antarctic Search for Meteorites (ANSMET) programme, which has been funded by NSF and NASA and characterized and curated by the Department of Mineral Sciences of the Smithsonian Institution and Astromaterials Acquisition and Curation Office at NASA JSC. A. Nguyen is thanked for her assistance with NanoSIMS operations at JSC. D. K. Ross is thanked for assistance with electron microprobe analysis at JSC.

Author contributions

F.M.M. and J.J.B. conceived the project. J.J.B., F.M.M. and A.R.S. collected electron beam data. J.J.B. collected and reduced all isotopic data. All authors contributed to the writing and to discussions and revision of the manuscript.

Competing interests

The authors declare no competing interests.

Additional information

Extended data is available for this paper at https://doi.org/10.1038/s41561-020-0552-y.

Supplementary information is available for this paper at https://doi.org/10.1038/s41561-020-0552-y.

Correspondence and requests for materials should be addressed to J.J.B.

Reprints and permissions information is available at www.nature.com/reprints.

Editor recognition statement Primary Handling Editor: Stefan Lachowycz.

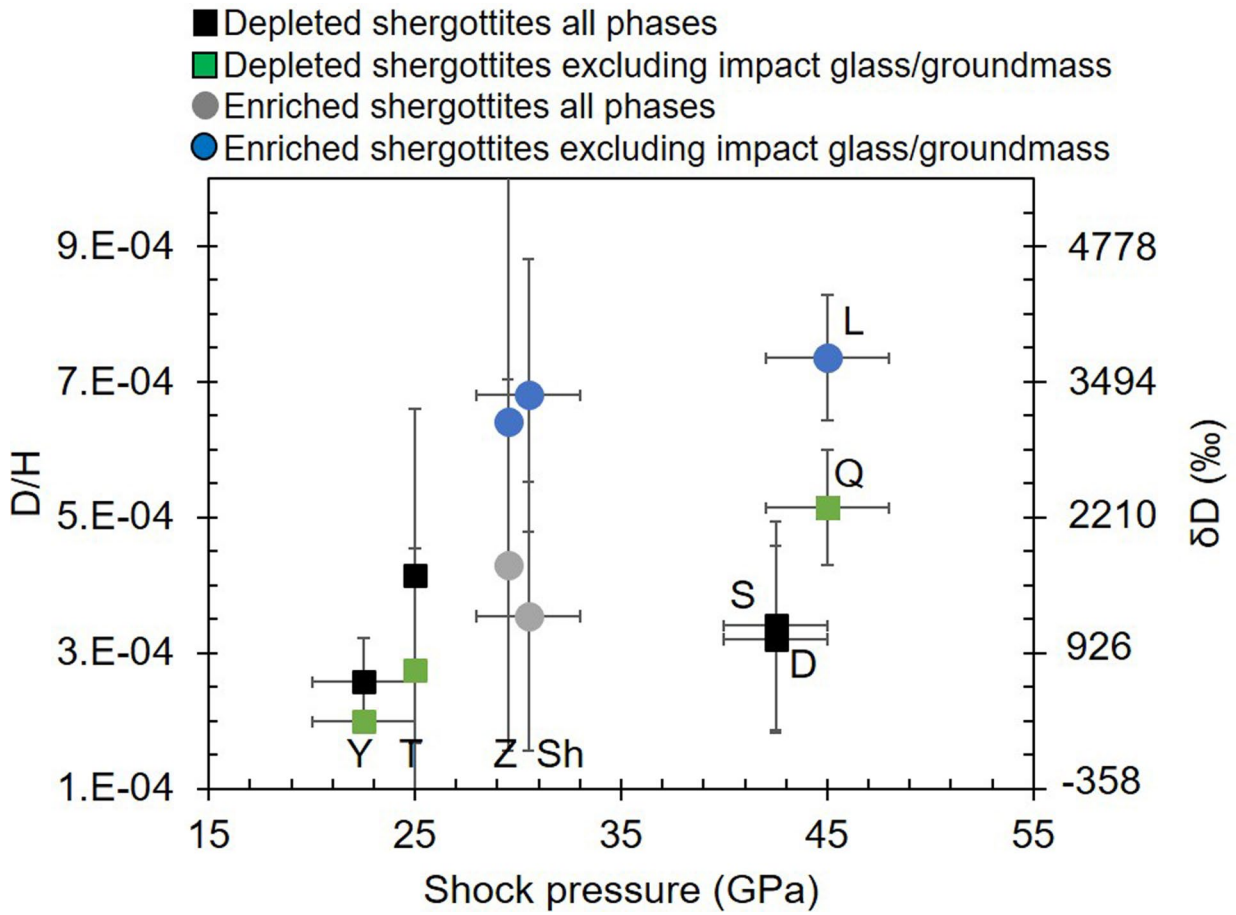

Extended Data Fig. 1 | Plot showing the average D/H for minerals and glasses versus shock pressure for shergottites. There is no apparent correlation between shergottite type and shock implantation of hydrogen. Where: Y = Yamato 980459, T = Tissint, Z = Zagami, Sh = Shergotty, S = Sayh al Uhaymir 005, D = Dar al Gani 005, Q = Queen Alexandra Range 94201, and L = Los Angeles. D/H data are compiled in Supplementary Table 2. Note that only non-impact glass/groundmass D/H reported from Q and L, and only feldspathic glass reported from S and D. Error bars represent standard deviation of the mean for D/H and the range in reported shock pressures[42,43].